

Synthesis and characterization of visible-light absorbing ordered mesoporous titanosilicate incorporated with vanadium oxide

In-Soo Park ^a, Sun Young Choi ^a, Jeong Sook Ha ^{a,*}, Jihyeong Khim ^b

^a Department of Chemical and Biological Engineering, Korea University, Anam-dong, Seongbuk-gu, Seoul 136-713, Republic of Korea

^b Department of Civil Engineering, Korea University, Anam-dong, Seongbuk-gu, Seoul 136-713, Republic of Korea

Received 13 February 2007; in final form 30 June 2007

Available online 7 July 2007

Abstract

Ordered mesoporous titanosilicates (OMTs) showing UV–visible-light absorption were synthesized using SBA-15 ordered mesoporous silica as a host framework, where the incorporated vanadium oxide worked as a visible-light receptor. The structures and the chemical composition of the OMTs were investigated with powder X-ray diffraction, nitrogen physisorption isotherm, transmission electron microscope and X-ray photoelectron spectroscopy. Vanadium oxide nanoparticles are incorporated into the interconnecting mesopores of SBA-15 structure and the most of titanium dioxide is uniformly coated on SBA-15 as well as vanadium oxide surfaces. The presence of vanadium oxide nanoparticles in OMTs induced visible-light absorption of titanium oxide at the wavelength above 400 nm.

© 2007 Elsevier B.V. All rights reserved.

1. Introduction

The photo-induced activation of titanium oxide (TiO₂) has attracted significant interest during the last decade in the energy conversion for Grätzel cell, photooxidation of pollutants, self-cleaning surfaces and super hydrophilic surfaces [1–4]. Among the photo-activities of TiO₂, the photocatalytic degradation of organic molecules has been found to be a very effective method on the removal of organic pollutants in waste water [2–5]. However, ordinary TiO₂ is activated only by UV light of wavelength shorter than 400 nm, which limits the use of sun light in photocatalytic degradation [6]. In order to enhance the absorption edge at visible-light region, the incorporation of light-sensitizing modifiers, such as Cr, V, Fe ions and other semiconductors, in TiO₂ was examined [2,4,5,7]. In addition to broad-band absorption of TiO₂, enlarged surface area for TiO₂ is preferable since the photoactivated degradation of organics occurs only on the surface of TiO₂ catalyst [2–8].

Since the first report on the well-ordered mesoporous silica designated as M41S was reported in the early 1990s [9], ordered mesoporous silica materials invoked tremendous applications utilizing their various pore connectivity, high specific surface area, large pore volume, controllable pore size and facile incorporation of guest molecules into the pore [10]. Among the ordered mesoporous silica materials, SBA-15 is a noticeable material that is synthesized by triblock copolymer as a structure-directing agent and silica sources in acidic conditions [11]. The SBA-15 has two-dimensionally ordered hexagonal array with *P6mm* symmetry of uniform mesopores in the range of 5–20 nm, narrow pore size distribution, large surface area, large pore volume and better thermal–hydrothermal stability than the first mesoporous silica, MCM-41 [12,13].

Taking advantage of such ordered mesoporous silica, the ordered mesoporous TiO₂ based on SBA-15 structure has been extensively examined for several years [14,15]. However, the majorities of ordered mesoporous titanosilicates (OMTs) have dealt with pure TiO₂ on porous silica materials which have the photo activity only in UV-light range. Recently, there was a report on the visible-light absorbing titanosilicates synthesized by Cr³⁺ ion doping into TiO₂ on SBA-15 silica framework [16]. Here, we report

* Corresponding author. Fax: +82 2 926 6102.

E-mail address: jeongsha@korea.ac.kr (J.S. Ha).

on the synthesis and structural investigation of novel OMTs with vanadium oxide as a visible-light receptor. Such synthesized OMTs showed a large specific surface area with broad-band absorption of UV–visible-light and the ordered structure with TiO_2 .

2. Experimental

SBA-15 was synthesized following the procedure reported by Choi et al. [17] except for the use of 5% sodium silicate solution and hydrothermal treatment condition. The sodium silicate solution was prepared by dissolution of colloidal silica (Ludox LS, 30 wt% SiO_2 , Aldrich) using 0.64 M NaOH under mild heating, and the sodium silicate solution was added to the aqueous solution of P123 (Aldrich) in 0.3 M HCl with stirring at 35 °C, continued for 24 h at the same temperature. The mixture was placed into an autoclave and heated in an oven at 150 °C for 24 h. The SBA-15 product was filtered and dried at 70 °C. To remove the organic surfactant, the product was washed with a mixture of ethanol and HCl, and calcined further at 550 °C for 2 h in air. Vanadyl sulphate hydrate ($\text{VOSO}_4 \cdot x\text{H}_2\text{O}$, $x \sim 5.06$, 99.99%, Aldrich) was introduced to calcined SBA-15 by incipient wetness technique using methanol, and then the vanadium oxide (V_2O_5 , ICDD number 41-1426) was generated inside SBA-15 by thermal degradation of vanadyl sulphate upon heating to 550 °C for 2 h. The relative molar ratio of Si to V, denoted as Si/V, was changed from ∞ to 20 by control of V content. To incorporate TiO_2 , 2.13 g of 50 wt% titanium(IV) butoxide (97%, Aldrich) solution in absolute ethanol (Merck) was infiltrated to 1.0 g of V_2O_5 containing SBA-15 below 0 °C, and then the ethanol was removed under

vacuum condition. The product was heated in an oven at 95 °C with water vapour to convert titanium precursors to TiO_2 . The final calcination was performed by heating to 450 °C over 4 h and maintained at the same temperature for 3 h in air.

Powder X-ray diffraction (XRD) patterns were obtained by Rigaku DMax-2200 Ultima series operated with Cu $K\alpha$ radiation at 1.6 kW. Nitrogen physisorption isotherms were obtained with a Micromeritics ASAP 2010 instrument at -196 °C. The specific surface area was calculated by the BET equation, using the data in the P/P_0 region between 0.05 and 0.15 [18]. The pore size distribution was estimated by standard Barrett–Joyner–Halenda (BJH) method [19]. The sum of micropore and mesopore volumes were estimated by the α_s plot method by extrapolating the α_s values in the ranges from 1.9 to 2.3 where the α_s values were converted by using the report of Jaroniec et al. [20]. For transmission electron microscopy (TEM), porous carbon grid was dipped into the dispersion of powdered sample in ethanol using ultrasonication. TEM images were obtained using a JEOL JEM-3010 instrument with EDS attachment, which was operated at 300 kV. X-ray photoelectron spectroscopy (XPS) data were collected using ThermoVG Sigma Probe. UV–visible spectra were obtained by using Shimadzu UV-3101PC model in a reflection mode.

3. Results and discussion

The XRD patterns of basal SBA-15 silica, vanadium oxide containing SBA-15 without TiO_2 (Si/V = 20, designated as VSBA-15 hereafter) and ordered mesoporous titanosilicates (OMTs) with various vanadium contents are shown in Fig. 1. XRD patterns below $2\theta = 3^\circ$ show distinct-

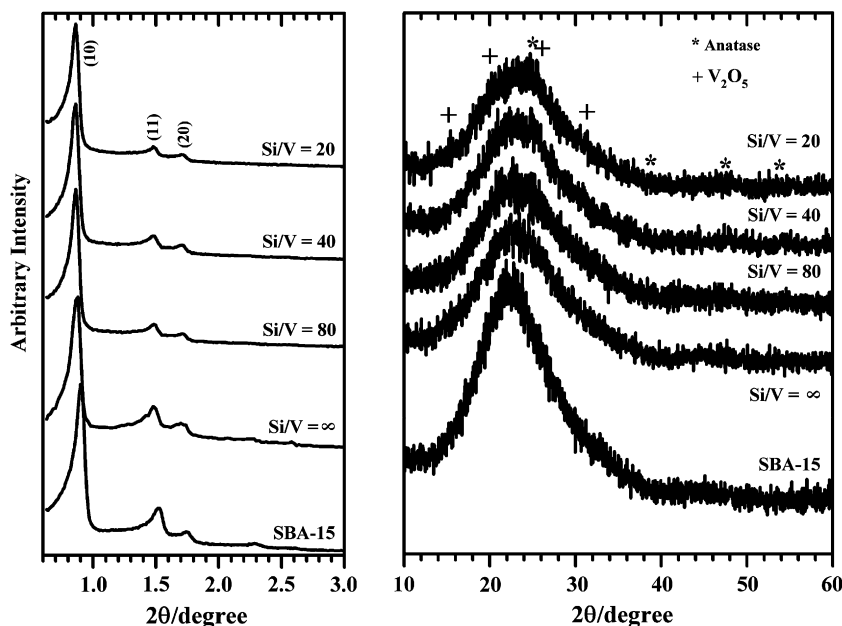


Fig. 1. XRD patterns of SBA-15 silica, VSBA-15 (Si/V = 20) and ordered mesoporous titanosilicates (OMTs) based on the SBA-15 with various vanadium contents. The Si/V denotes the ratio between silica and vanadium oxide in molar contents. The peak position corresponding to anatase TiO_2 and V_2O_5 (ICDD number 41-1426) are marked as * and +, respectively.

tive two-dimensionally ordered hexagonal structures with $P6mm$ symmetry for SBA-15, VSBA-15 and OMTs. There is almost no change of the SBA-15-based mesostructures after the TiO_2 incorporation except for the minor increase of lattice parameters and decrease of diffraction intensity (see Table 1 for the lattice parameter a_0 , estimated from the position of (10) diffraction peak). However, the origin of this minor lattice expansion after the inclusion of TiO_2 is not clear. The XRD patterns above 10° show no apparent peaks corresponding to crystalline anatase phase of TiO_2 and V_2O_5 except for the broad peak centered at 23° corresponding to amorphous silica and TiO_2 . It is tentatively considered that the TiO_2 and V_2O_5 are present as either crystalline phase with small domains or amorphous phase.

Adsorption–desorption isotherms of nitrogen measured at -196°C for SBA-15 and OMTs are presented in Fig. 2a and the detailed data are summarized in Table 1. The iso-

therms show representative type IV nitrogen physisorption curves and steep inflection in the range of $P/P_0 = 0.6\text{--}0.8$ corresponding to capillary condensation for mesoporous region. Although the BJH method always estimates smaller value than real pore size [21], it was applied here for the comparison of relative pore size distribution among the SBA-15, VSBA-15 and OMTs. The pore size distributions of OMTs from desorption branch by BJH method show the two distinct pores corresponding to open mesopore around 7.9 nm and partially blocked mesopore around 5.3 nm (see the inset of Fig. 2a). Introduction of TiO_2 induces the increase in the wall thickness (w) of OMTs since the V_2O_5 inside the interconnecting mesopores could decrease the room for TiO_2 . Therefore, the larger wall thickness was estimated with the higher contents of V_2O_5 as listed in Table 1. This implies a considerably uniform coating of TiO_2 on the silica walls. Accordingly, the gradual volume decrease of open mesopore with increase of

Table 1
Structural parameters for SBA-15 and OMTs, determined by XRD and N_2 physisorption isotherm^a

	a_0 (nm)	S_{BET} ($\text{m}^2 \text{g}^{-1}$)	D_{ads} (nm)	D_{des} (nm)	w (nm)	V_t ($\text{cm}^3 \text{g}^{-1}$)	$V_{\text{micro}} + V_{\text{meso}}$ ($\text{cm}^3 \text{g}^{-1}$)
SBA-15	11.3	402.8	11.6	8.0	3.3	0.91	0.82
VSBA-15	11.5	379.8	11.6	7.8	3.7	0.86	0.75
Si/V = ∞	11.7	291.4	7.2, 11.0	5.3, 7.9	3.8	0.55	0.49
Si/V = 80	11.8	275.8	7.0, 11.0	5.2, 7.9	3.9	0.52	0.46
Si/V = 40	11.9	272.1	7.0, 11.0	5.3, 7.9	4.0	0.51	0.45
Si/V = 20	11.9	271.6	7.0, 10.8	5.2, 7.8	4.1	0.51	0.40

^a a_0 , XRD unit cell parameter; S_{BET} , BET specific surface area deduced from the isotherm analysis in the relative pressure range from 0.05 to 0.15; D_{ads} , mesopore size calculated from adsorption branch using BJH method; D_{des} , mesopore size calculated from desorption branch using BJH method; w , wall thickness obtained by the subtraction of D_{des} from a_0 ; V_t , total pore volume at relative pressure of 0.95; ($V_{\text{micro}} + V_{\text{meso}}$), the sum of micropore and mesopore volume estimated from α_s plot with the range of $\alpha_s = 1.9\text{--}2.3$.

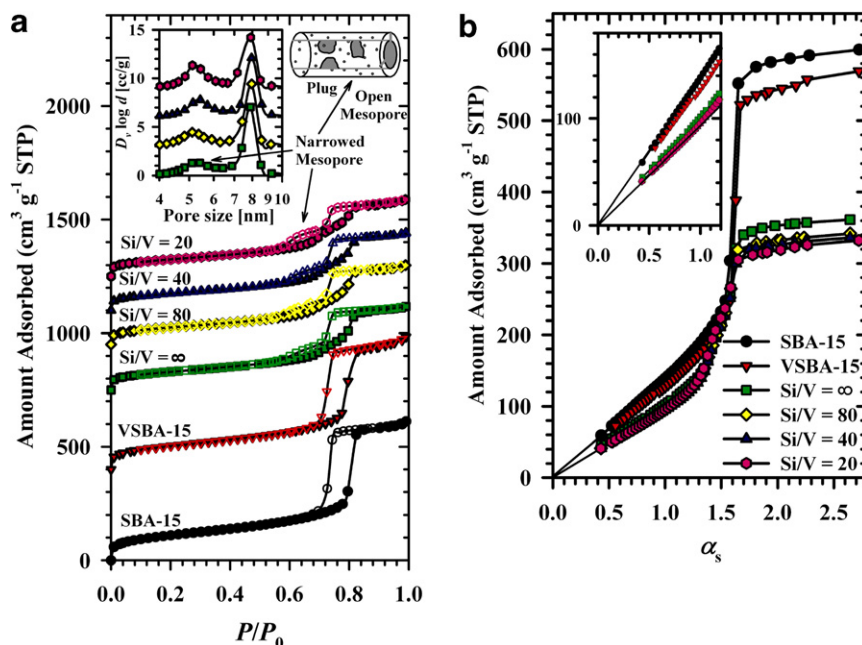


Fig. 2. (a) Nitrogen physisorption isotherms of SBA-15 and OMTs containing vanadium oxide. The samples are offset vertically to 0, 400, 750, 950, 1100 and $1250 \text{ cm}^3 \text{g}^{-1}$ STP, respectively. The inset denotes the pore size distribution deduced from BJH method using desorption branch of each isotherms. (b) α_s plot analysis for SBA-15 and OMTs deduced from the nitrogen adsorption isotherms. The inset shows the magnified α_s plot at the low α_s values.

vanadium oxide content is attributed to the partial blockage of open mesopores by the introduction of vanadium oxide. However, the existence of partially blocked mesopore corresponding to 5.3 nm also implies the partial inhomogeneity of TiO_2 coating. The BET specific area (S_{BET}) and total pore volume (V_t) continuously also decreased with increasing vanadium oxide content; hence, the increase in the amount of vanadium oxide results in more blockages of the mesopores in OMTs.

The characteristics of pores, such as micro-mesopore volume and external surface area, are usually estimated by α_s plot [22]. The α_s plot is obtained by using isotherm data of nonporous standard reference to eliminate the surface binding factors between adsorbate and substrate. Fig. 2b shows the α_s plots for SBA-15, VSBA-15 and OMTs which are obtained from N_2 physisorption data in Fig. 2a. The extrapolated intersections at $\alpha_s = 0$ converge to zero with linear extension; thus, the surface characteristics seem to be similar after the introduction of TiO_2 , and there seems to be rare microporosity in the SBA-15, VSBA-15 and OMTs [20]. The SBA-15 that was hydrothermally treated at temperatures above 130°C exhibited noticeable decrease of interpenetrating micropores in silica wall, whereas the large interconnecting pores between mesopores were generated [23]. The sum of micropore and mesopore volumes ($V_{\text{micro}} + V_{\text{meso}}$) also decreases gradually with increasing vanadium oxide content, in accordance with the trend observed in S_{BET} and V_t .

TEM images taken from the OMT with $\text{Si}/\text{V} = 20$ are shown in Fig. 3. TEM images display the regular stripe patterns originated from SBA-15, and their pore diameter and the lattice spacing (a_0) are measured to be about 8 nm and 12 nm, respectively; thus, the structural parameters are consistent with XRD and N_2 physisorption results. The irregular contrast of OMT pore walls is observed along the pore directions, where the darker area is placed on the interconnections between the three-way center of mesopores as clearly shown in Fig. 3b. Since the darker area in TEM images represents the electronically more dense

phases, the vanadium oxide is considered to be highly probable phase in the interconnecting mesopores. Furthermore, the low melting point (690°C) of anhydrous V_2O_5 may result in the lowering of melting point when the nano-sized V_2O_5 are placed in confined structures; consequently, the nano-sized V_2O_5 can be placed in narrower interconnecting mesopores during the V_2O_5 generation process at 550°C [24]. In addition, TEM-EDS results estimated the molar ratio of Ti and V to be 4.1 (Ti/V) in large extent of OMTs.

The chemical composition of vanadium in OMTs was confirmed by XPS as shown in Fig. 4. Both peaks centered

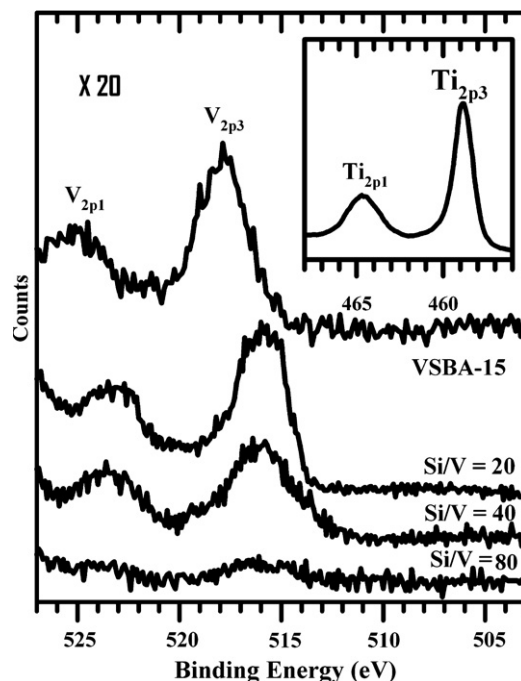


Fig. 4. XPS spectra of vanadium in VSBA-15 and OMTs with different vanadium oxide contents. The inset shows the XPS spectrum of titanium in OMTs with $\text{Si}/\text{V} = 20$.

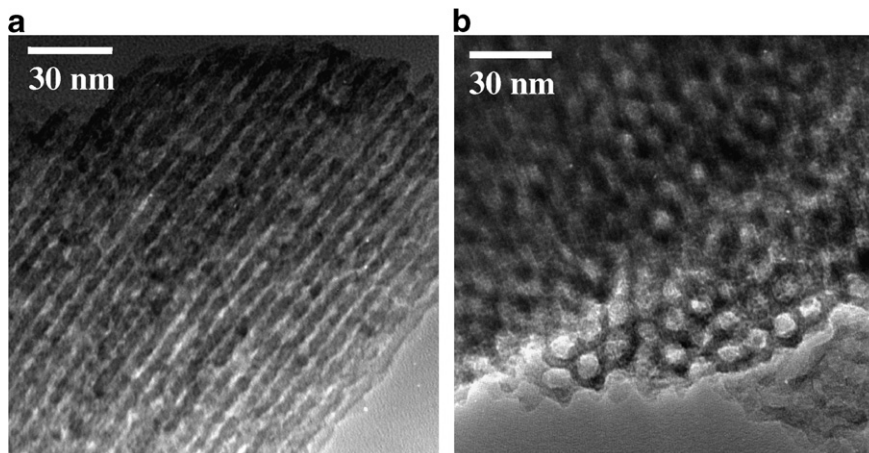


Fig. 3. TEM images of OMT with $\text{Si}/\text{V} = 20$: (a) side view and (b) vertical view.

at 516.1 and 523.6 eV are attributed to be $V2p^1$ and $V2p^3$ of V_2O_5 , respectively [25]. However, their binding energy values are lower than 518.0 and 524.9 eV for referenced values of V_2O_5 in VSBA-15, respectively, probably because the electropositive TiO_2 layers are coated on V_2O_5 nanoparticles. The XPS spectrum for Ti in OMT with Si/V = 20, as shown in the inset of Fig. 4, exhibits relatively higher binding energy of 458.9 eV compared to 458.6 eV for TiO_2 catalysts [25].

Optical properties of OMTs were examined by taking the UV–visible spectra, as shown in Fig. 5. The OMT without vanadium oxide (Si/V = ∞) shows only UV absorption at the wavelengths below 400 nm. However, the incorporation of vanadium oxide in OMTs exhibits visible-light absorption at the wavelength above 400 nm and its intensity increased with the increase of vanadium oxide content. The absorption band at ~ 420 nm is contributed from the heterojunction between TiO_2 and V^{5+} ion as reported in $TiO_2/V-Ti-MCM-41$ system and the large amount of vanadium oxide results in relatively high absorption intensity compared to $TiO_2/V-Ti-MCM-41$ system [26]. The absorption band at the wavelength above ~ 560 nm is interpreted as optical band gap energy of 2.0–2.2 eV, which is responsible for V^{5+} species in crystalline V_2O_5 itself as shown for VSBA-15 [27]. These results are similar to those of TiO_2 included V–Ti–MCM-41 system [26]. Therefore, the photo-activity of OMTs using visible-light can be expected. Since the mesoporous titanosilicate using SBA-15 is considered to have the larger accessible pore than MCM-41, the wider applications to the photocatalytic deg-

radation of pollutants including large reactant molecules as well as small ones are expected. Their practical application to the oxidation reactions with visible-light is under investigation.

4. Conclusion

Visible-light absorbing ordered mesoporous titanosilicates were successfully synthesized by sequential incorporation of vanadium oxide and titanium oxide into hexagonally ordered mesoporous silica, SBA-15. Vanadium oxide is considered to exist as V_2O_5 nanoparticles in the interconnecting mesopores of SBA-15, and TiO_2 is coated on SBA-15 silica as well as V_2O_5 nanoparticles. The UV–visible spectra show that the presence of V_2O_5 enables TiO_2 to absorb the visible-light. The visible-light absorbing photocatalysts with various pore dimensions other than SBA-15 structure may be fabricated in this way and they will have promising applications such as photocatalyst for selective oxidation reactions.

Acknowledgements

This work was supported by the Ministry of Science and Technology (Grant No. M10503000187-05M0300-18710), National Research Laboratory Program of the Korean Science and Engineering Foundation and Korea Research Foundation (Grant No. KRF-2004-005-C00068).

References

- [1] M. Grätzel, *Nature* 414 (2001) 338.
- [2] T.L. Thompson, J.T. Yates, *Chem. Rev.* 106 (2006) 4428.
- [3] A. Fujishima, T.N. Rao, D.A. Tryk, *J. Photochem. Photobiol. C* 1 (2002) 1.
- [4] D.G. Shchukin, D.V. Sviridov, *J. Photochem. Photobiol. C* 7 (2006) 23.
- [5] M.R. Hoffmann, S.T. Martin, W. Choi, D.W. Bahnemann, *Chem. Rev.* 95 (1995) 69.
- [6] D.F. Ollis, *Environ. Sci. Technol.* 19 (1985) 480.
- [7] M. Anpo, in: M. Kaneko, I. Okura (Eds.), *Photocatalysis: Science and Technology*, Kodansha, Tokyo, 2002, p. 175.
- [8] A.L. Linsebigler, G. Lu, J.T. Yates Jr., *Chem. Rev.* 95 (1995) 735.
- [9] C.T. Kresge, M.E. Leonowicz, W.J. Roth, J.C. Vartuli, J.S. Beck, *Nature* 359 (1992) 710.
- [10] A. Stein, *Adv. Mater.* 15 (2003) 763.
- [11] D. Zhao, J. Feng, Q. Huo, N. Melosh, G.H. Fredrickson, B.F. Chmelka, G.D. Stucky, *Science* 279 (1998) 548.
- [12] U. Ciesla, F. Schüth, *Micropor. Mesopor. Mater.* 27 (1999) 131.
- [13] M. Kruk, M. Jaroniec, C.H. Ko, R. Ryoo, *Chem. Mater.* 12 (2000) 1961.
- [14] Z. Luan, E.M. Maes, P.A.W. Heide, D. Zhao, R.S. Czernuszewicz, L. Kevan, *Chem. Mater.* 11 (1999) 3680.
- [15] R. Grieben, J. Aguado, M.J. López-Muñoz, J. Marugán, *J. Photochem. Photobiol. A: Chem.* 148 (2002) 315.
- [16] B. Sun, E.P. Reddy, P.G. Smirniotis, *J. Catal.* 237 (2006) 314.
- [17] M. Choi, W. Heo, F. Kleitz, R. Ryoo, *Chem. Commun.* (2003) 1340.
- [18] S. Brunauer, P.H. Emmet, E. Teller, *J. Am. Chem. Soc.* 60 (1938) 309.
- [19] E.P. Barret, L.G. Joyner, P.P. Hanenda, *J. Am. Chem. Soc.* 73 (1951) 373.
- [20] M. Jaroniec, M. Kruk, J.P. Olivier, *Langmuir* 15 (1999) 5410.

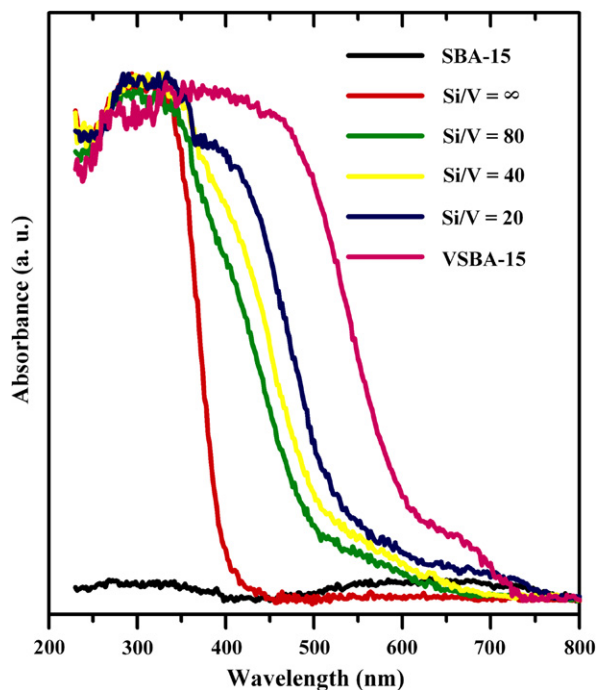


Fig. 5. UV–visible spectra for SBA-15, VSBA-15 and OMTs with variation of vanadium oxide content.

- [21] P.I. Ravikovitch, A.V. Neimark, *J. Phys. Chem. B* 105 (2001) 6817.
- [22] K. Kaneko, C. Ishii, M. Ruike, H. Kuwabara, *Carbon* 30 (1992) 1075.
- [23] A. Galarneau, H. Cambon, F.D. Renzo, R. Ryoo, M. Choi, F. Fajula, *New J. Chem.* 27 (2003) 73.
- [24] I.-S. Park, J.S. Ha, unpublished result.
- [25] C.D. Wagner, W.M. Riggs, L.E. Davis, J.F. Moulder, G.E. Muilenberg, *Handbook of X-ray Photoelectron Spectroscopy*, Perkin-Elmer Corporation, 1978.
- [26] E.P. Reddy, L. Davydov, P.G. Smirniotis, *J. Phys. Chem. B* 106 (2002) 3394.
- [27] V. Eyert, K.-H. Höck, *Phys. Rev. B* 57 (1998) 12727.